Arabidopsis SH3P2 is an ubiquitin-binding protein that functions together with ESCRT-I and the deubiquitylating enzyme AMSH3

Marie-Kristin Nagel[a,b], Kamila Kalinowska[b,1], Karin Vogel[a,b], Gregory D. Reynolds[c], Zhixiang Wu[d], Franziska Anzenberger[b], Mie Ichikawa[e], Chie Tsutsumi[f], Masa H. Sato[e], Bernhard Kuster[d], Sebastian Y. Bednarek[c], and Erika Isono[a,b,2]

[a]Chair of Plant Physiology and Biochemistry, Department of Biology, University of Konstanz, 78457 Konstanz, Germany; [b]Chair of Plant Systems Biology, School of Life Sciences Weihenstephan, Technical University of Munich, 85354 Freising, Germany; [c]Department of Biochemistry, University of Wisconsin–Madison, Madison, WI 53706; [d]Chair of Proteomics and Bioanalytics, School of Life Sciences Weihenstephan, Technical University of Munich, 85354 Freising, Germany; [e]Department of Life and Environmental Sciences, Kyoto Prefectural University, 606-0823 Kyoto, Japan; and [f]Department of Botany, National Museum of Nature and Science, 305-0005 Tsukuba, Japan

Edited by Natasha V. Raikhel, Center for Plant Cell Biology, Riverside, CA, and approved July 17, 2017 (received for review June 17, 2017)

Clathrin-mediated endocytosis of plasma membrane proteins is an essential regulatory process that controls plasma membrane protein abundance and is therefore important for many signaling pathways, such as hormone signaling and biotic and abiotic stress responses. On endosomal sorting, plasma membrane proteins maybe recycled or targeted for vacuolar degradation, which is dependent on ubiquitin modification of the cargos and is driven by the endosomal sorting complexes required for transport (ESCRTs). Components of the ESCRT machinery are highly conserved among eukaryotes, but homologs of ESCRT-0 that are responsible for recognition and concentration of ubiquitylated proteins are absent in plants. Recently several ubiquitin-binding proteins have been identified that serve in place of ESCRT-0; however, their function in ubiquitin recognition and endosomal trafficking is not well understood yet. In this study, we identified Src homology-3 (SH3) domain-containing protein 2 (SH3P2) as a ubiquitin- and ESCRT-I–binding protein that functions in intracellular trafficking. SH3P2 colocalized with clathrin light chain-labeled punctate structures and interacted with clathrin heavy chain *in planta*, indicating a role for SH3P2 in clathrin-mediated endocytosis. Furthermore, SH3P2 cofractionates with clathrin-coated vesicles (CCVs), suggesting that it associates with CCVs *in planta*. Mutants of *SH3P2* and *VPS23* genetically interact, suggesting that they could function in the same pathway. Based on these results, we suggest a role of SH3P2 as an ubiquitin-binding protein that binds and transfers ubiquitylated proteins to the ESCRT machinery.

ubiquitin | ESCRT | DUB | clathrin | *Arabidopsis*

Plants are constantly facing environmental changes, and are therefore forced to readily respond and adapt to the environment for optimal growth and reproduction. Plasma membrane receptors and transporters play an essential role in the coordination of extracellular signals and intracellular responses. Regulation of the activity and abundance of signaling molecules at both transcriptional and posttranscriptional levels is therefore key to all important signaling pathways, such as phytohormone signaling and biotic and abiotic stress responses (1–3). The clathrin-mediated endosomal sorting and degradation pathway is responsible for the degradation of many plasma membrane proteins and is conserved in eukaryotes (4–6). The binding and polymerization of clathrin triskelia in concert with adaptor protein complexes at the plasma membrane result in the budding and release of plasma membrane cargo protein-containing clathrin-coated vesicles (CCVs) that deliver their cargo to the trans-Golgi network (TGN)/early endosomal compartment (EE) (5). From there, the internalized plasma membrane proteins can either be transported by intracellular vesicle trafficking to the vacuole for degradation or recycled back to the plasma membrane (3).

Vacuolar degradation of plasma membrane proteins is dependent on posttranslational modification by ubiquitin, or ubiquitylation. Ubiquitin can be conjugated into different chain types, and depending on the type of linkage, these chain types target the modified proteins to different cellular degradation pathways (7). Ubiquitin chains linked at the internal lysine 63 (K63) can serve as a transport signal for endocytic trafficking and selective autophagy (7, 8). In plants, degradation of membrane proteins, such as the auxin efflux carrier PIN-FORMED 2 (PIN2) and the brassinosteroid receptor BRASSINOSTEROID INSENSITIVE 1 (BRI1), was shown to depend on K63-linked ubiquitin chain modification (9, 10). The abundance of the plasma membrane transporters IRON-REGULATED TRANSPORTER 1 (IRT1) and REQUIRES HIGH BORON 1 (BOR1) is also controlled by ubiquitin-dependent endocytic degradation in response to nutrient availability in the environment (11, 12). Some pathogens also use ubiquitylation as a mechanism to remove host defense proteins. The bacterial effector AvrPtoB has ubiquitin ligase activity and ubiquitylates the host FLAGELLIN-SENSITIVE (FLS) 2 and CHITIN ELICITOR RECEPTOR KINASE (CERK) 1, the removal of which is advantageous for the bacteria (13, 14).

Ubiquitin-mediated sorting of cargo proteins from the plasma membrane is driven by the endosomal sorting complexes required for transport (ESCRTs); ESCRT-0, ESCRT-I, ESCRT-II, and

Significance

The endosomal sorting of integral proteins is essential for controlling signaling pathways at the plasma membrane. Posttranslational modification by ubiquitin is key to proper degradation of plasma membrane proteins as the ubiquitylated transmembrane proteins are recognized by multiple ubiquitin adaptor proteins and trafficked to the vacuole for degradation. Although plants lack orthologs of the yeast and metazoan endosomal sorting complex required for transport-0 heterodimer that functions as an ubiquitin adaptor, plants appear to have evolved other strategies to recognize and concentrate ubiquitylated proteins that have been endocytosed. Here, we report the SH3P2 protein as a yet-unknown ubiquitin adaptor protein in *Arabidopsis* and its molecular function in regulating the endocytic transport and degradation.

Author contributions: M.-K.N., K.K., B.K., S.Y.B., and E.I. designed research; M.-K.N., K.K., K.V., G.D.R., Z.W., F.A., C.T., and E.I. performed research; M.I. and M.H.S. contributed new reagents/analytic tools; M.-K.N., K.K., K.V., G.D.R., Z.W., C.T., B.K., S.Y.B., and E.I. analyzed data; and M.-K.N. and E.I. wrote the paper.

The authors declare no conflict of interest.

This article is a PNAS Direct Submission.

[1]Present address: Chair of Cell Biology and Plant Biochemistry, Biochemie-Zentrum, University of Regensburg, Regensburg, Germany.

[2]To whom correspondence should be addressed. Email: erika.isono@uni-konstanz.de.

This article contains supporting information online at www.pnas.org/lookup/suppl/doi:10.1073/pnas.1710866114/-/DCSupplemental.

ESCRT-III (3, 15). The ESCRT machinery is highly conserved in eukaryotes, and, besides playing a central role in intracellular trafficking (16), it was shown in other organisms to be involved in viral budding (17, 18) and membrane reformation and repair (19–23). The ESCRT machinery was shown to be important in many physiological aspects of plant biology (3). Of the four types of ESCRT machinery (ESCRT-0, ESCRT-I, ESCRT-II, and ESCRT-III), plants lack ESCRT-0. ESCRT-0, a heterodimer of two ubiquitin-binding proteins, Vps27p/Hrs and Hse1/signal-transducing adaptor molecule (STAM), is important for concentrating and trapping ubiquitylated membrane cargos and passing them to ESCRT-I. ESCRT-I and ESCRT-II also contain ubiquitin-binding subunits, which are important for keeping the ubiquitylated cargos on the endosomal membranes en route to the vacuole for degradation (24). ESCRT-III interacts with ESCRT-II and is responsible for the scission of membranes and the formation of intraluminal vesicles during the maturation of multivesicular bodies (MVBs) (16).

Ubiquitin recognition is key for the ESCRT-dependent intracellular trafficking pathway. All ESCRTs, except for ESCRT-III, and many ESCRT-related proteins contain ubiquitin-binding domains, and many of these proteins can interact with each other, thereby increasing their affinity toward ubiquitylated cargos (16, 25). Additional protein families that mediate recognition of ubiquitylated cargo proteins have been identified and shown to direct ubiquitylated cargos to the ESCRT machinery (24). The ubiquitin adaptor proteins, Golgi-localized, γ-ear–containing ADP ribosylation factor-binding proteins (GGAs), are present in both mammals and yeast, but not in plants, whereas TARGET OF MYB (TOM) 1 proteins appear in metazoans and have homologs in plants (24, 26). GGAs and TOM1 interact with ESCRT-I and send the cargo to the ESCRT-mediated protein degradation route (27, 28).

Although plants lack GGA homologs (3, 15), nine TOM-LIKEs (TOLs) are encoded in the *Arabidopsis* genome (26). TOLs were shown to bind ubiquitylated proteins and to localize to the plasma membrane and intracellular punctate structures, and they are necessary for endocytosis and recycling of the auxin efflux carrier PIN2 (26). Fab1, YOTB, Vac1, and EEA (FYVE) domain-containing protein 1 (FYVE1)/FYVE DOMAIN PROTEIN REQUIRED FOR ENDOSOMAL SORTING 1 (FREE1) is another ubiquitin-binding protein in *Arabidopsis* that interacts and colocalizes with ESCRT-I, and is important for intracellular trafficking and degradation of ubiquitylated proteins (29–32). For a better understanding as to how the recognition and condensation of ubiquitylated cargo proteins work in plant cells, it is necessary to uncover the molecular framework in which ubiquitin-binding proteins and ESCRT-I function.

In this work, we demonstrate that the *Arabidopsis* Src homology-3 (SH3) domain-containing protein 2 (SH3P2) can act as an ubiquitin-binding protein and functions together with ESCRT-I and the deubiquitylating enzyme (DUB) associated molecule with the SH3 domain of STAM3 (AMSH3). *Arabidopsis* has three homologs that are named SH3P1, SH3P2, and SH3P3. Besides the C-terminal SH3 domain, the SH3Ps contain a putative N-terminal BIN-amphiphysin-RVS (BAR) domain (33), a domain present in membrane-associated proteins that are involved in clathrin-mediated endocytosis. SH3Ps bind phosphoinositides, and SH3P1 and SH3P2 localize on clathrin-labeled structures, indicating that these proteins are involved in intracellular trafficking (32–35). Our data show that SH3P2 interacts with the ESCRT-I subunit VPS23 and binds K63-linked ubiquitin chains, and also the DUB AMSH3. SH3P2, VPS23, and the DUB AMSH3 all localize to punctate structures labeled by the clathrin marker. Moreover, *VPS23* and *SH3P2* show genetic interactions, suggesting that they could function together. Based on these results, we propose a role for SH3P2 in the recognition of ubiquitinated membrane cargos and in passing them to the ESCRT machinery for degradation.

Results

SH3P2 Binds K63-Linked Ubiquitin Chains. To establish whether there are other ubiquitin adaptors in the plant endocytosis pathway, we investigated proteins that were reported to localize on the plasma membrane or CCVs for putative ubiquitin-binding motifs. We focused on the SH3Ps since SH3 domains were previously reported to bind ubiquitin (36–38). There are three homologs of SH3Ps (SH3P1, SH3P2, and SH3P3) that seem to be distributed early in evolution of dicots (Fig. S1). Of these three homologs, SH3P1 and SH3P2 were reported to localize on clathrin-positive vesicles (32, 34).

We first examined whether the SH3 domain of SH3P2 has the ability to bind ubiquitin and ubiquitin conjugates, and examined full-length SH3P2 and fragments of SH3P2 with and without the SH3 domain (Fig. 1*A*) in an ubiquitin-binding assay. Full-length SH3P2 binds to K63-linked ubiquitin chains but does not bind linear or K48-linked tetra-ubiquitin (Fig. 1*B*). Further experiments show that an SH3P2 fragment containing the SH3 domain binds K63-linked tetra-ubiquitin, whereas a fragment deleted of the SH3 domain did not show binding (Fig. 1*C*). GST-SH3P2 (SH3) also bound to ubiquitin conjugates from plant total extracts, whereas GST alone did not (Fig. 1*D*). These data suggest that the SH3 domain of SH3P2 can bind ubiquitin and has a preference toward the K63-linkage type.

SH3P2 Interacts with ESCRT-I. The function of ubiquitin adaptors in endocytosis is to concentrate ubiquitinated cargos and to transfer them to the ESCRT machinery, especially ESCRT-I. We therefore investigated whether SH3P2 interacts with ESCRT-I components. ESCRT-I consists of three core subunits, VPS37,

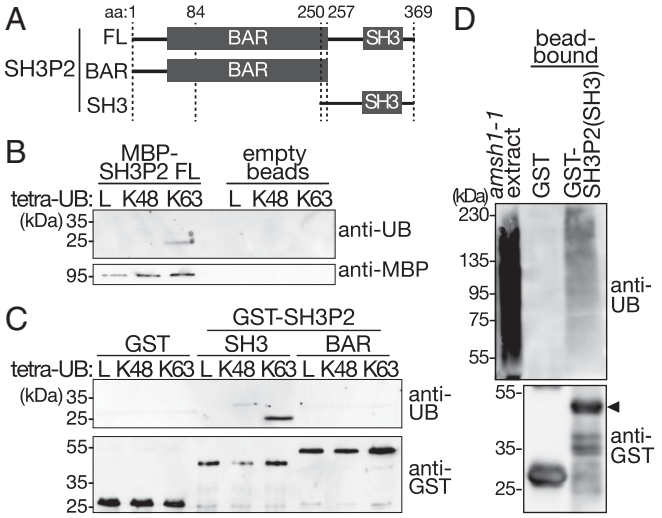

Fig. 1. SH3P2 binds ubiquitin conjugates. (*A*) Schematic presentation of full-length SH3P2(FL) and truncation constructs SH3P2(BAR) and SH3P2(SH3) used in *C* and *D*. (*B*) Tetra-ubiquitin (UB)–binding assay with recombinant MBP-SH3P2. Equal amounts of bead-bound MBP-SH3P2(FL) and linear (L), K48-linked (K48), or K63-linked (K63) tetra-UB were incubated together. After washing, the binding of tetra-UB to MBP-SH3P2(FL) was analyzed by immunoblotting with anti-UB (P4D1) and anti-MBP antibodies. Empty amylose beads were used as a negative control. (*C*) Tetra-UB–binding assay with GST-SH3P2(SH3) and GST-SH3P2(BAR). Equal amounts of bead-bound GST-SH3P2(SH3), GST-SH3P2(BAR), and GST were incubated with L, K48, or K63 tetra-UB. After washing, the binding of tetra-UB to the GST-fusion proteins was analyzed by immunoblotting with anti-UB (P4D1) and anti-GST antibodies. (*D*) UB-binding assay with GST-SH3P2(SH3) and GST. Bead-bound recombinant GST-SH3P2(SH3) and GST were incubated with crude extracts of *amsh1-1*. After washing, bead-bound materials were subjected to immunoblotting with anti-UB (P4D1) and anti-GST antibodies. The arrowhead indicates the position of GST-SH3P2(SH3).

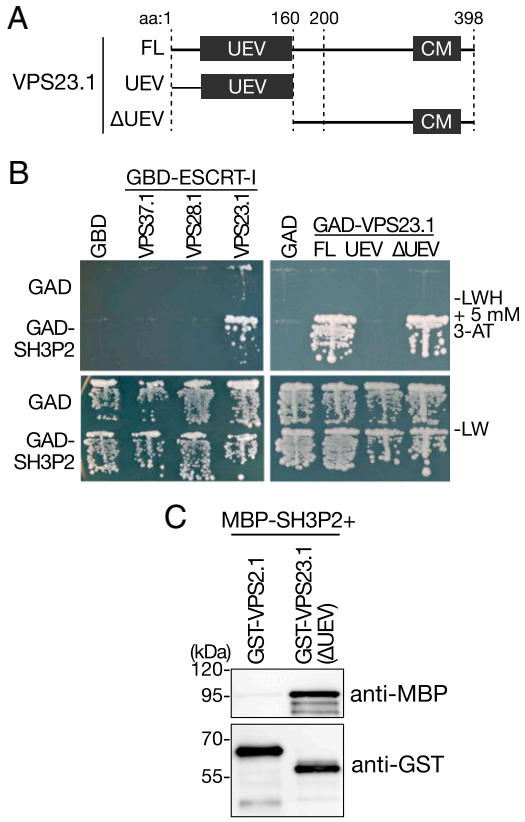

Fig. 2. SH3P2 interacts directly with VPS23.1. (*A*) Schematic presentation of full-length VPS23.1(FL) and truncated constructs VPS23.1(UEV) and VPS23.1 (ΔUEV) used for YTH and in vitro assays in *B* and *C*. (*B*) YTH analysis of GAD-SH3P2 with GBD-fusions of ESCRT-I subunits GBD-VPS37.1, GBD-VPS28.1, and GBD-VPS23.1, and YTH analysis of GBD-SH3P2 with GAD-fused VPS23.1(FL), VPS23.1(UEV), and VPS23.1(ΔUEV). Yeast transformants were grown on media lacking leucine and tryptophan (−LW) or leucine, tryptophan, and histidine (−LWH) supplemented with 5 mM 3-amino-1,2,4-triazole (3-AT) to test their auxotrophic growth. Empty vectors, GAD and GBD, were used as negative controls. The expression of all fusion proteins was verified by immunoblotting shown in Fig. S2 *A* and *B*. (*C*) In vitro-binding assay of SH3P2 with VPS23.1(ΔUEV). The ESCRT-III subunit VPS2.1 was used as a negative control. Bead-bound GST-VPS2.1 and GST- VPS23.1(ΔUEV) were incubated with equal amounts of full-length MBP-SH3P2. After intensive washing, bead-bound materials were subjected to immunoblotting using anti-MBP and anti-GST antibodies.

VPS28, and VPS23, and *Arabidopsis* has two homologs for each subunit. We tested one of each of the homologs and examined the interaction of GAD-SH3P2 against GBD-fused VPS23.1, VPS28.1, and VPS37.1 in a yeast two-hybrid (YTH) analysis. VPS23.1 has an N-terminal ubiquitin E2 variant (UEV) domain that is a conserved ubiquitin-binding domain and a C-terminal core motif (Fig. 2*A*). SH3P2 showed YTH interaction with only VPS23.1 (Fig. 2*B* and Fig. S2*A*). A targeted YTH analysis and an in vitro-binding assay have shown that the UEV domain is dispensable for this interaction (Fig. 2 *B* and *C* and Fig. S2*B*).

Immunoelectron microscopic analysis has previously shown that SH3P1, a homolog of SH3P2, localizes on the plasma membrane, the TGN, and the CCVs associated with them (34). We have previously shown that SH3P2 localizes on clathrin light chain (CLC)-labeled punctate structures and on late-endosome–associated aggregates that appear upon blockage of ESCRT-III disassembly (32). The ESCRT-I subunit VPS28 was previously demonstrated by immunoelectron microscopic analysis to localize on the TGN (39). However, colocalization of ESCRT-I subunits with clathrin markers has not been established *in planta*. We therefore generated plants expressing *VPS23.1-TagRFP* under the endogenous promoter and analyzed the localization with endosomal markers, including YFP-CLC (clathrin), GFP-SYP43 (TGN/EE) (40), and YFP-ARA7 (PVC/MVBs) (41) (Fig. 3*A*), as well as with SH3P2-superfolder GFP (sGFP) (32) (Fig. 3*B*). VPS23.1-TagRFP localized on punctate structures and colocalized with another ESCRT-I subunit, GFP-VPS28.1, when both were expressed under their native promoters (Fig. S3). Colocalization efficiency analysis showed that VPS23.1-TagRFP punctate structures showed the highest level of colocalization (52.3%, $n = 241$) with YFP-CLC (Fig. 3 *A* and *C*), whereas only 4.6% ($n = 304$) and 4.4% ($n = 248$) of the VPS23.1-TagRFP vesicles showed colocalization with the GFP-SYP43 and ARA7-labeled early and late endosomes, respectively (Fig. 3*C*). We could not detect localization of VPS23.1-TagRFP on the plasma membrane or on cell plates. When crossed with an SH3P2-sGFP

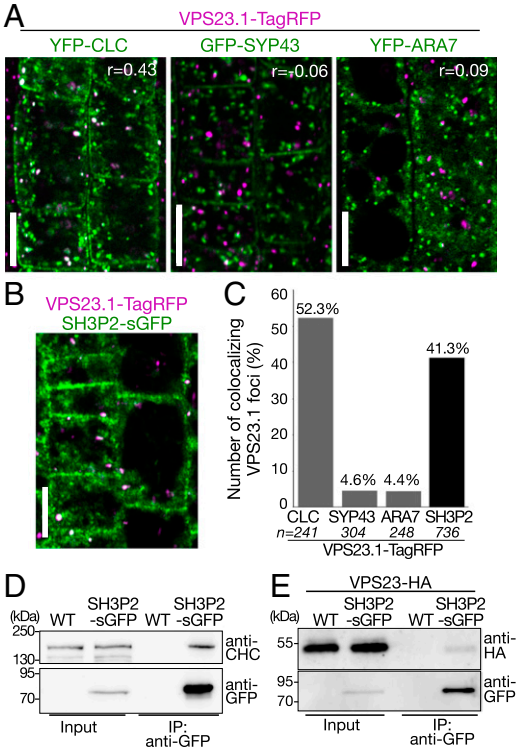

Fig. 3. VPS23.1-TagRFP colocalizes with SH3P2-sGFP and YFP-CLC *in planta*. (*A*) Colocalization analysis of VPS23.1-TagRFP with endosomal markers. Colocalization of VPS23.1-TagRFP with the clathrin marker YFP-CLC (*Left*), the early endosome marker GFP-SYP43 (*Center*), and the late endosome marker YFP-ARA7 (*Right*) was analyzed with a confocal microscope in root epidermis cells of 7-d-old *Arabidopsis* seedlings. *r*, Pearson's correlation coefficient. (Scale bars: 10 μm.) (*B*) Colocalization of VPS23.1-TagRFP and SH3P2-sGFP. The localization of VPS23.1-TagRFP and SH3P2-sGFP in root epidermis cells of 7-d-old seedlings was analyzed under a confocal microscope. (Scale bar: 10 μm.) (*C*) Percentage of VPS23.1-TagRFP–positive foci that colocalize with endosomal markers or SH3P2-sGFP shown in *A* and *B*. *n*, total numbers of analyzed VPS23.1-TagRFP foci. (*D*) CHC coimmunoprecipitates with SH3P2-sGFP. Total extracts of 7-d-old wild-type (WT) and SH3P2-sGFP–expressing seedlings were incubated with anti-GFP antibody-immobilized agarose. After intensive washing, bead-bound materials [immunoprecipitated (IP) material: anti-GFP] and total extracts (input) were subjected to immunoblotting using anti-CHC and anti-GFP antibodies. (*E*) VPS23.1-HA coimmunoprecipitates with SH3P2-sGFP. Total extracts of WT and SH3P2-sGFP seedlings expressing VPS23.1-HA were incubated with anti-GFP antibody-immobilized agarose. After intensive washing, the IP material (anti-GFP) was subjected to immunoblots together with the total extracts (input) using anti-HA and anti-GFP antibodies.

line, 41.3% (n = 736) of the VPS23.1-TagRFP foci colocalized with SH3P2-sGFP–positive foci (Fig. 3 *B* and *C*).

Next, we investigated whether SH3P2 and ESCRT-I can interact in vivo. Total extracts were prepared from wild-type and *SH3P2pro:SH3P2-sGFP* seedlings and mixed with GFP-trap beads. Immunoblots using anti-GFP and anti-clathrin heavy chain (CHC) antibodies showed that the endogenous CHC was coimmunoprecipitated with SH3P2-sGFP (Fig. 3*D*). Similarly, VPS23.1-HA was also specifically coimmunoprecipitated with SH3P2-sGFP (Fig. 3*E*). Taken together, these data show that both VPS23.1 and SH3P2 colocalize with CLC, suggesting that they can function together on intracellular clathrin-positive organelles *in planta*. The fact that SH3P2-sGFP interacts with both CHC and VPS23.1-HA in vivo suggests that these proteins can function together in the intracellular trafficking pathway.

SH3P2 Is Associated with CCVs. To further establish whether SH3P2 is localized on CCVs, we purified CCVs from 7-d-old seedlings expressing SH3P2-GFP under the native promoter using a tandem fractionation scheme based on differential and density centrifugation (42). SH3P2-GFP cofractionated with CHC, and was retained in the purified CCV fraction, whereas other organelle or compartment markers did not (Fig. 4*A*), indicating that SH3P2 is associated with CCVs.

SH3P2 was previously reported to bind phospholipids, and it was shown that the BAR domain alone was sufficient for this binding (33–35). Accordingly, we observed that the truncated protein without the complete BAR domain SH3P2(ΔNBAR: amino acids 179–369)-sGFP did not localize on the plasma membrane or on intracellular punctate structures, whereas the localization of SH3P2(BAR: amino acids 1–257)-sGFP was indistinguishable from that of the full-length fusion protein (FL) (Fig. 4*B*). SH3P2(ΔNBAR)-sGFP also lost its interaction with CHC (Fig. 4*C*), indicating that the N-terminal region containing the BAR domain is indispensable for the interaction with membrane structures containing clathrin and for the localization of SH3P2 on the plasma membrane and on clathrin-positive foci.

SH3P2 Interacts with the DUB AMSH3. Since the DUB AMSH was initially identified as a protein that interacts with the SH3 domain of STAM, an ESCRT-0 subunit in mammals (43), we investigated whether the *Arabidopsis* AMSH3 and SH3P2 can directly interact. As shown in Fig. 5*A*, MBP-SH3P2 bound to GST-AMSH3 but not to GST-VPS2.1, an ESCRT-III subunit that served as a negative control, showing that AMSH3 interacts with SH3P2 in vitro (Fig. 5*A*). However, the addition of SH3P2 in a DUB assay using AMSH3 did not show altered activity of AMSH3 (Fig. S4), indicating that SH3P2 does not influence the in vitro DUB activity of AMSH3.

To establish whether AMSH3 has a function in clathrin-mediated endocytosis, we explored the interaction of AMSH3 with other proteins reported to function in the pathway. Like SH3P2, AMSH3 was found to interact with the ESCRT-I subunit VPS23.1 in an YTH assay (Fig. 5*B* and Fig. S5) and in an in vitro-binding assay (Fig. 5*C*). In addition, VPS23.1-HA and AMSH3 were coimmunoprecipitated from total protein extracts of *Arabidopsis* seedlings (Fig. 5*D*), suggesting that these proteins function together in vivo. AMSH3 was previously shown to localize on ARA6- and ARA7-labeled late endosomes (44). To analyze whether AMSH3 can also localize together with VPS23.1 on clathrin-labeled foci, we analyzed the colocalization between AMSH3-YFP and CLC-monomeric Kusabira Orange (mKO). Forty-nine percent of AMSH3-YFP foci colocalized with CLC-mKO (n = 398; Fig. 5*E*). To investigate whether AMSH3-YFP foci showed distinct localization with CLC- and ARA7-labeled endosomes, seedlings expressing AMSH3-YFP, CLC-mKO, and ECFP-ARA7 were examined. A total of 40.4% of AMSH3-YFP signals colocalized with endosomes labeled with ECFP-ARA7,

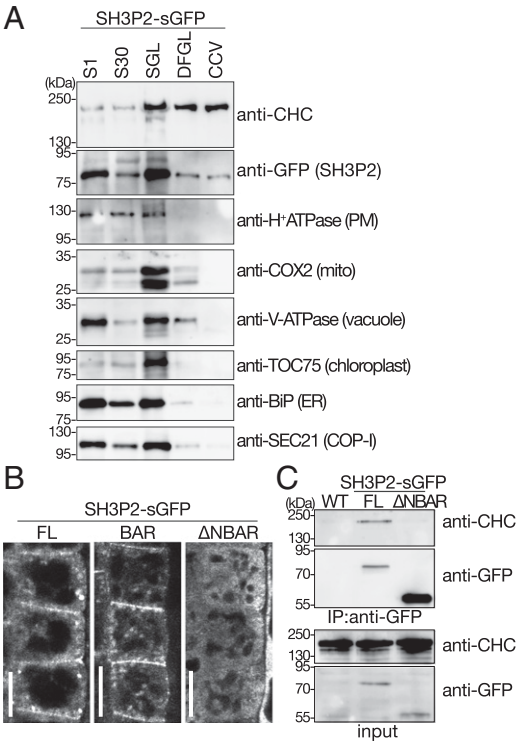

Fig. 4. SH3P2 fractionates with the CCV fraction. (*A*) CCVs were prepared from total plant extract of 7-d-old seedlings. Samples were collected during the procedure of CCV purification and subjected to Western blot analyses using antibodies against CHC, GFP, and various subcellular organelle marker proteins. CCV, CCV-containing fraction; DFGL, linear deuterium oxide/Ficoll gradient load; S1, supernatant after 1,000 × *g* centrifugation; S30, supernatant after 30,000 × *g* centrifugation; SGL, sucrose step gradient load. The following antibodies were used as organelle- or compartment-specific markers: anti–H^+-ATPase [plasma membrane (PM)], anti-COX2 [mitochondria (mito)], anti–V-ATPase (vacuole), TOC75 (chloroplast), anti-BiP [endoplasmic reticulum (ER)], and anti-SEC21 [COP-I vesicle (COP-1)]. (*B*) Localization of full-length SH3P2-sGFP(FL), SH3P2-sGFP(BAR), and SH3P2-sGFP(ΔNBAR). Localization was analyzed in the root epidermis cells of 7-d-old seedlings by confocal microscopy. Whereas the GFP-fused SH3P2-sGFP(FL) and SH3P2-sGFP(BAR) localized to the PM and on intracellular punctate structures, SH3P2-sGFP(ΔNBAR) signals are dispersed in the cytosol. (Scale bars: 10 μm.) (*C*) Immunoprecipitation of full-length SH3P2-sGFP(FL) and SH3P2-sGFP(ΔNBAR). Full-length SH3P2-sGFP(FL) and SH3P2-sGFP(ΔNBAR) were immunoprecipitated from total extracts prepared from 8-d-old seedlings expressing the respective constructs. The bead-bound material (IP material: anti-GFP) and total extracts (input) was subjected to immunoblotting using anti-GFP and anti-CHC antibodies.

28.3% of AMSH3-YFP signals colocalized with CLC-mKO, and 14.5% of the AMSH3-YFP signals colocalized with both markers (Fig. 5 *F* and *G*). These results indicate that CLC-mKO and ARA7-YFP predominantly reside on separate compartments and that AMSH3-YFP is associated with both CLC- and ARA7-labeled endosomes. To verify the independence of the CLC-mKO and ECFP-ARA7 in this line, we treated seedlings with the PI3K/PI4K inhibitor Wortmannin (WM). ECFP-ARA7 localized to the typical swollen late endosomal compartments induced by WM, whereas CLC-mKO did not (Fig. 5*F*), indicating the two markers maintain largely distinct localization patterns even upon coexpression of AMSH3-YFP. Taken together, these data show that VPS23.1, AMSH3, and SH3P2 all localize on CLC-positive punctate structures and likely function together in plants.

***SH3P2* Shows Genetic Interactions with the ESCRT-I Subunit *VPS23.1*.** To investigate the physiological role of SH3P2 in *Arabidopsis*, we examined transfer-DNA (T-DNA) insertion lines of *SH3P1*,

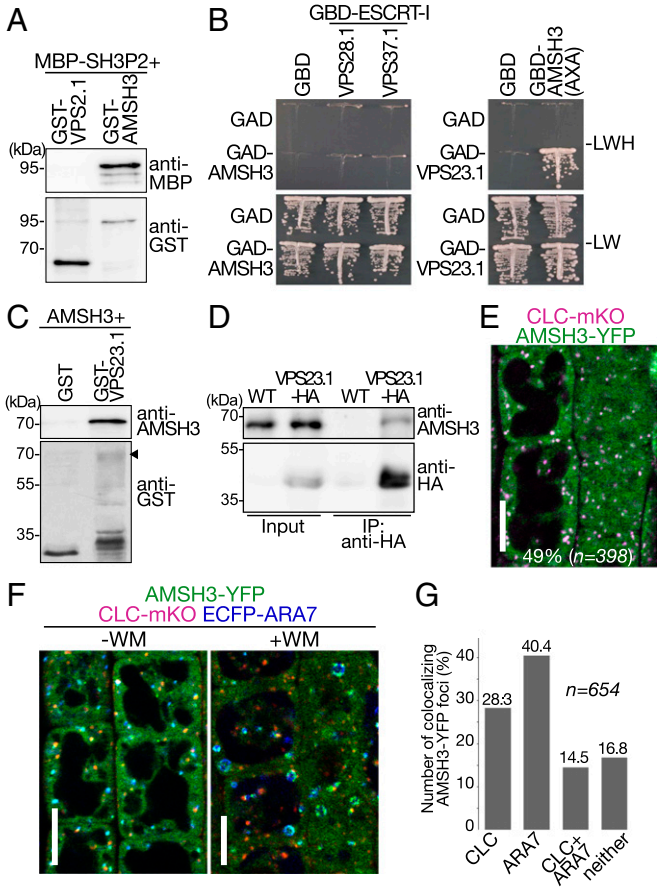

Fig. 5. DUB AMSH3 interacts directly with SH3P2 and VPS23.1 and localizes on both CLC- and ARA7-positive endosomes. (*A*) In vitro-binding assay of SH3P2 with AMSH3. Bead-bound GST-AMSH3 and the negative control GST-VPS2.1 were incubated with equal amounts of full-length MBP-SH3P2. After intensive washing, bead-bound materials were analyzed by immunoblotting with anti-MBP and anti-GST antibodies. (*B*) YTH analysis of AMSH3 with ESCRT-I subunits. GAD-AMSH3 or GBD-AMSH3(AXA) was coexpressed with ESCRT-I subunits GBD-VPS28.1, GBD-VPS37.1, and GAD-VPS23.1. Yeast transformants expressing both GAD- and GBD-fusions were grown on media lacking leucine and tryptophan (−LW) or leucine, tryptophan, and histidine (−LWH) to test their auxotrophic growth. Empty vectors were used as negative controls. The expression of fusion proteins was verified by immunoblotting, as shown in Fig. S5. (*C*) In vitro-binding assay of AMSH3 with VPS23.1. Bead-bound GST-VPS23.1 was incubated with an equal amount of AMSH3. After intensive washing, bead-bound materials were analyzed by immunoblotting with anti-AMSH3 and anti-GST antibodies. The arrowhead indicates the position of GST-VPS23.1. (*D*) AMSH3 coimmunoprecipitates with VPS23.1-HA. Total extracts of wild-type (WT) and VPS23.1-HA seedlings were incubated with anti-HA antibody-immobilized agarose. After intensive washing, the immunoprecipitated (IP) material (anti-HA) was subjected to immunoblotting together with the total extracts (input) using anti-HA and anti-AMSH3 antibodies. (*E*) Colocalization of AMSH3-YFP and CLC-mKO. The localization of AMSH3-YFP and CLC-mKO in root epidermis cells of 7-d-old seedlings was analyzed under a confocal microscope. (Scale bar: 10 μm.) (*F*) Colocalization of AMSH3-YFP with CLC-mKO and ECFP-ARA7. The localization was analyzed under a confocal microscope in root epidermis cells of 7-d-old seedlings expressing AMSH3-YFP with CLC-mKO and ECFP-ARA7 without (*Left*) or with 60 min of WM treatment (*Right*). (Scale bars: 10 μm.) (*G*) Percentage of AMSH3-YFP foci that colocalize with CLC only, ARA7 only, with both CLC and ARA7, or with neither marker (without WM treatment). *n*, total number of analyzed AMSH3-YFP foci.

SH3P2, and *SH3P3* and identified null mutant alleles designated *sh3p1* and *sh3p3* (Fig. S6 *A* and *B*). For *SH3P2*, we could not identify any T-DNA insertion lines that affected the level of *SH3P2* transcript, and therefore generated an artificial microRNA (amiRNA) line designated *amish3p2*, which has a 90% reduction in the level of *SH3P2* mRNA relative to wild type and the *sh3p1sh3p3* double mutant (Fig. S6*C*).

Neither the *sh3p1sh3p3* double mutant nor *amish3p2* showed apparent developmental phenotypes (Fig. S6*D*) even in the presence of the ARF-GEF inhibitor Brefeldin A (BFA) (Fig. S6*E*). In addition, uptake of the endocytosis tracer FM4-64 in *amish3p2* was comparable to wild-type seedlings (Fig. S6*F*). As SH3P2 was reported to be involved in autophagy, we next tested the *amish3p2* for dark-induced autophagy phenotypes. The mutants remained indistinguishable from the wild type even after prolonged dark treatment, whereas *atg7*, a bona fide autophagy defective mutant, displayed pale green leaves and significantly reduced chlorophyll content (Fig. S6*G*). Repeated attempts to generate a *sh3p1sh3p3amish3p2* triple mutant failed, as the amiRNA construct did not express in the *sh3p1sh3p3* double-mutant background, and thus we cannot rule out the existence of redundancy between the three *SH3Ps*.

To test whether mutants of *vps23* and *sh3p2* show genetic interactions, we first established mutants of *vps23*. *Arabidopsis* has two *VPS23* homologs, *VPS23.1/VPS23A/ELCH* and *VPS23.2/VPS23B/ELCH-LIKE*. We isolated T-DNA insertion mutants of *VPS23.1* and *VPS23.2* that we named *vps23.1-3* and *vps23.2-1*, both of which were null mutants (Fig. S7 *A* and *B*). We then crossed them with each other to generate double mutants. We could not recover double-homozygous mutants among the progeny of a double-heterozygous plant, suggesting that the double-homozygous mutants are not viable. The inviable phenotype of the double homozygotes was rescued by the expression of *VPS23.1:VPS23.1-TagRFP* (Fig. S7*C*), indicating that the VPS23 function is essential in *Arabidopsis* and that the *VPS23.1-TagRFP* construct used for the localization studies was functional.

We also observed that 9.6% of the total progenies of *vps23* double-heterozygous plants were smaller than their siblings and had small cotyledons. PCR-based genotyping identified them as *vps23.1-3*$^{-/-}$*vps23.2-1*$^{+/-}$ (Fig. 6*A*, Table 1, and Fig. S7*D*). The phenotypes could be further divided according to the color of the cotyledons. A total of 8.6% of progenies had small but green cotyledons (Table 1 and Fig. S7*D*), while 1% of progenies remained white even when grown in light, suggesting that these mutants have defects in greening in addition to developmental defects. In progenies from a wild-type plant, none of the seedlings showed this phenotype (Table 1). In the progeny of a *vps23.1-3*$^{+/-}$*vps23.2-1*$^{+/-}$ line harboring the *amish3p2* construct, the number of seedlings with small white cotyledons significantly increased to 4.7% (Fig. 6*A* and Table 1), while the number of seedlings with small green cotyledons decreased to 5.8%, indicating that the presence of *amish3p2* increased the number of *vps23.1-3*$^{-/-}$*vps23.2-1*$^{+/-}$ seedlings with greening defects. To verify that this shift is caused by *amish3p2*, we generated an amiRNA-resistant variant of *SH3P2-sGFP* named *SH3P2*(*amiRNAres*)*-EGFP*, and introduced it into the *vps23.1-3*$^{+/-}$*vps23.2-1*$^{+/-}$*amish3p2* background. *SH3P2*(*amiRNAres*)*-EGFP* restored the segregation of seedling phenotypes (Table 1), confirming the effect of *amish3p2* on the *vps23* mutants. The expression of *SH3P2*(*amiRNAres*)*-EGFP* was verified under confocal microscopy (Fig. S7*E*).

Recently, it has been reported that VPS23.1 is involved in the ubiquitin-dependent degradation of the abscisic acid (ABA)-receptor PYR1-like 4 (PYL4) in *Arabidopsis* (45). Upon treatment with ABA, a null mutant of *vps23.1* (*vps23a*) accumulated ubiquitylated proteins, while the level of ubiquitin conjugates was indistinguishable from the wild type when untreated. To test whether the *vps23.1-3*$^{-/-}$*vps23.2-1*$^{+/-}$ mutant shows defects in ubiquitin-mediated protein degradation, we examined the ubiquitin profile of mutant seedlings. Seven-day-old seedlings with mutant phenotypes accumulated ubiquitinated proteins at a high level (Fig. 6*B*), indicating that VPS23 is required for the removal of ubiquitin conjugates also in ABA-independent processes.

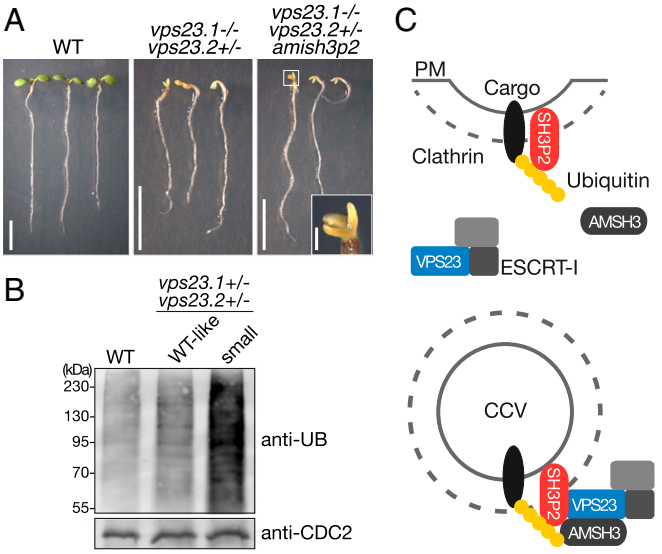

Fig. 6. The *vps23.1-3*$^{-/-}$*vps23.2-1*$^{+/-}$ seedlings show severe developmental defects and accumulate ubiquitylated proteins. (*A*) Phenotypes of *vps23.1-3*$^{-/-}$*vps23.2-1*$^{+/-}$ seedlings. Photographs of 7-d-old wild type (WT; *Left*), *vps23.1-3*$^{-/-}$*vps23.2-1*$^{+/-}$ (*Center*), and *vps23.1-3*$^{-/-}$*vps23.2-1*$^{+/-}$ harboring the *amish3p2* construct (*Right*) are shown. (*Right Inset*) Among the *vps23.1-3*$^{-/-}$*vps23.2-1*$^{+/-}$*amish3p2* seedlings, seedlings with tricotyledons were also found. (Scale bars: 5 mm; *Inset*, 0.5 mm.) (*B*) Accumulation of ubiquitin (UB) conjugates in *vps23* mutants. Total protein extracts of 7-d-old WT, *vps23.1-3*$^{-/-}$*vps23.2-1*$^{+/-}$ WT-looking progenies (WT-like siblings), and aberrant *vps23.1-3*$^{-/-}$*vps23.2-1*$^{+/-}$ (small) seedlings were subjected to immunoblotting using an anti-UB antibody. Note that *vps23.1-3*$^{-/-}$*vps23.2-1*$^{+/-}$ (small) seedlings accumulate ubiquitylated proteins compared with the WT seedlings. Anti-CDC2 antibody was used as a loading control. (*C*) Possible function of SH3P2 on CCVs. SH3P2 can bind to the K63-linked ubiquitin chain of a cargo protein at the plasma membrane (PM) and, through its BAR domain, can bind to the membrane during clathrin-mediated endocytosis of ubiquitylated cargo proteins. SH3P2 could recruit ESCRT-I to the CCV via the interaction with the subunit VPS23. VPS23 binds the ubiquitin chain of the endocytosed cargo and leads the cargo to the downstream ESCRT machinery. The DUB AMSH3 can bind both the SH3P2 and the ESCRT-I subunit VPS23 and could be recruited by both proteins to the CCVs. Deubiquitylated membrane cargos might be recycled back to the PM.

Taken together, previous data (34, 35) and the data presented in this study suggest that *Arabidopsis* ESCRT-I VPS23.1, AMSH3, and SH3P2 localize and function together on clathrin-labeled endomembrane structures. SH3P2 can bind K63-linked ubiquitin chains of membrane proteins in close proximity to the plasma membrane or on/in CCVs. We propose a model (Fig. 6*C*) in which SH3P2 binds ubiquitylated cargos at the plasma membrane and during clathrin-mediated endocytosis. Alternatively, SH3P2 could be also recruited separately to the plasma membrane and to CCVs. SH3P2 could enrich ubiquitylated cargos at the endosomal membrane and, by interacting with VPS23, could pass them to the ESCRT machinery. On CCVs, SH3P2 could function together with the ESCRT-I subunit VPS23 and the DUB AMSH3. Since SH3P2 localizes to the plasma membrane, whereas VPS23 and AMSH3 do not, SH3P2 could also have an ESCRT-I– and DUB-independent function at the plasma membrane. Deubiquitylation of cargos by DUBs at this stage might rescue the cargo from being sorted into the ESCRT-dependent degradation pathway.

Discussion

SH3 domains can be found in all eukaryotes, and whereas more than 100 SH3 domain-containing proteins regulate diverse signaling pathways in mammals (46, 47), *Arabidopsis* has only five SH3 domain proteins, suggesting a different regulatory mechanism by SH3 domain proteins in animals and plants. In this work, we have demonstrated that the plant-specific SH3 domain-containing protein SH3P2 from *Arabidopsis* binds preferentially K63-linked ubiquitin chains and interacts in vitro and in vivo with the ESCRT-I subunit VPS23.1. SH3P2 interacts also with the DUB AMSH3. SH3P2, VPS23.1, and AMSH3 all localize on clathrin-positive intracellular structures. Based on these results, we propose a role for SH3P2 in the recognition of ubiquitinated cargos that are to be sorted into the ESCRT pathway.

Among proteins involved in membrane trafficking of plants, FYVE1/FREE1, ALG-2-interacting protein X (ALIX), TOLs, VPS23.1, and the ESCRT-II subunit VPS36 were shown to have affinity toward ubiquitin and/or ubiquitin chains in *Arabidopsis* (26, 30, 44, 48, 49). The lack of any obvious phenotypes in the *sh3p* mutants, despite the well-established importance of the ESCRT-mediated degradation pathway, could be due to the genetic redundancy between members of the *SH3P* family as well as other plant ubiquitin adaptor proteins. SH3P2 was recently reported to interact with the ubiquitin-binding FYVE1/FREE1 protein (30, 32), suggesting that ubiquitin-binding proteins may interact and function together. This may increase their affinity to ubiquitin chains and could enhance the efficiency of sorting the cargos into the ESCRT-dependent endocytic degradation pathway.

Polyubiquitylation of membrane proteins by ubiquitylating enzymes is key for the determination of protein stability (50, 51). By hydrolyzing the ubiquitin chains, DUBs could rescue the target proteins from degradation and recycle part of the cargos back to the plasma membrane. The recycling of membrane proteins can fine-tune the regulation of protein abundance at the plasma membrane and could also enable a faster reaction upon environmental changes without the cost for de novo protein synthesis.

Some DUBs require interacting proteins for their enzymatic activation (52). AMSH proteins, however, display DUB activity in vitro as monomers, although human AMSH proteins were reported to show higher activity in the presence of the interactor of AMSH, STAM (52). STAM is an SH3 domain-containing protein and ESCRT-0 subunit. The interaction between AMSH and SH3 domain-containing proteins seems to be conserved in plants, albeit the absence of ESCRT-0 and the structural differences between SH3P2 and STAM. Ubiquitin-binding proteins could facilitate the access of DUBs to the ubiquitin chain by simultaneously binding both the ubiquitin chain and the DUBs. In a quantitative in vitro DUB assay, however, preincubation of AMSH3 with SH3P2 did not accelerate the DUB activity of AMSH3. The acceleration of DUB activity may require different substrates or additional factors. AMSH3 lacks recognizable membrane-binding motifs, and thus is probably dependent on binding partners, such as ALIX, for its recruitment to endosomes (44). SH3P2 binds phospholipids (34, 35) and could also play a role in stabilizing the association of AMSH3 with endosomal membranes and the ESCRT machinery.

Table 1. Segregation of *vps23* mutant progenies

Genotype of mother plant	Normal seedlings, %	Small seedlings		*n*	χ^2 *P**
		Green, %	White, %		
Wild type (Col-0)	100.0	0	0	292	0.0050
vps23.1-3$^{+/-}$*vps23.2-1*$^{+/-}$	90.5	8.6	1.0	629	—
vps23.1-3$^{+/-}$*vps23.2-1*$^{+/-}$ *amish3p2*	89.5	5.8	4.7	551	0.0007
vps23.1-3$^{+/-}$*vps23.2-1*$^{+/-}$ *amish3p2* *SH3P2-sGFP*(*amiRNAres*)	87.1	10.9	2.0	248	0.4184

Col-0, Columbia-0.
*Compared with *vps23.1-3*$^{+/-}$*vps23.2-1*$^{+/-}$.

To date, only single mutants of ESCRT-I components have been analyzed in plants. The analyzed mutants of *VPS23.1*/*VPS23A*/*ELCH*, *VPS28.1*, and *VPS37.1* were all viable, but were defective in cytokinesis, endosomal sorting, and degradation of membrane-localized proteins and showed an altered phytohormone or pathogen response (45, 48, 53). The fact that the double-null mutant *vps23.1-3*$^{-/-}$*vps23.2-1*$^{-/-}$ displayed embryo lethality, shows that ESCRT-I, like ESCRT-III, is essential for plant growth and development. Similar to previously reported ESCRT-III mutants or ESCRT-III–related mutants, including *fyve1* and *amsh3* (30, 32, 44, 54), part of *vps23.1-3vps23.2-1* seedlings are small and have white cotyledons. Although the exact molecular mechanisms are unknown, a previous report has shown that mutants defective in membrane trafficking or plants treated with inhibitors of membrane trafficking have defects in plastid development (55). The mutant phenotypes observed in this study suggest that defects in ESCRT-I function may also have a similar effect on plastid development.

Localization studies have revealed similar but distinct localization patterns of ubiquitin-binding proteins in *Arabidopsis*. TOLs are predominantly localized to the plasma membrane, with a fraction on punctate structures in the cytosol (26), whereas FYVE1 and ALIX were not found at the plasma membrane, but were shown to localize on punctate structures that were colabeled with late endosomal markers (30, 32, 44). Our data, together with a previous report (34), demonstrate that the SH3Ps are associated with CCVs and localize on the plasma membrane, cell plate, and clathrin-positive foci. These localization studies suggest that ubiquitin adaptors, including SH3P2, can be involved in vesicle trafficking at diverse membrane compartments. Clathrin has been shown to form non-triskelia flat plaques on endosomal membranes, where it is assumed to be involved in the recruitment of ubiquitylated cargos together with ubiquitin-binding proteins (56–58). Whether SH3P2 could also interact and function together with clathrin on similar structures on the endosomes has yet to be elucidated.

While this paper was in preparation, Ahn et al. (35) reported that SH3P2 localizes to the tubulovesicular network at the cell plate and could function together with DYNAMIN RELATED PROTEIN (DRP) 1A during cell plate formation. It was also shown that SH3P2 binds phosphoinositides through its N-terminal BAR domain and that the BAR domain of SH3P2 can cause tubulation of liposomes (35). Future studies should reveal whether SH3P2 is also involved in membrane bending and/or scission events at the plasma membrane together with the DRPs and how the dynamics of SH3P2, ESCRT-I, and other ubiquitin-binding proteins are regulated during endocytosis.

Materials and Methods

Biological Material. All experiments were performed with *Arabidopsis thaliana* Columbia-0 (Col-0) background, except for the ELCH-HA line, which is in Wassilewskija-2 (Ws2) background (59). T-DNA insertion mutants *sh3p1* (Salk_127258), *sh3p3* (Salk_065790), *vps23.1-3* (Sail_1233E07_2-4) and *vps23.2-1* (Sail_237G05_3-4) were obtained from the Nottingham *Arabidopsis* Stock Centre.

Plant transformations were performed using the floral dip method (60). Plants were grown in continuous light or under long-day (16-h light/8-h dark) conditions with 100–120 $\mu mol \cdot m^{-2} \cdot s^{-1}$ light on Murashige and Skoog medium (MS; Duchefa Biochemie) supplemented with 1% sucrose germination media (GM). For root length measurements, seedlings were grown 6 d on GM supplemented with 3 μM BFA. For artificial starvation, 7-d-old seedlings grown on half-strength MS were transferred to the dark for 6 d.

Protein Purification, in Vitro-Binding Assays, and Ubiquitin-Binding Assay. GST- or MBP-fused proteins were expressed in the *Escherichia coli* Rosetta (DE3), Rosetta-gami 2, or Rosetta-gami B strains (all from Merck Millipore) and purified using Pierce Glutathione Magnetic Beads (Thermo Scientific), ProtinoGlutathione Agarose 4B (Macherey–Nagel), or Amylose Resin (New England Biolabs), depending on the fusion protein.

For in vitro-binding assays, Pierce Glutathione Magnetic Beads saturated with 25, 50, or 65 pmol of GST-fusion proteins were incubated with an equimolar amount of another protein or tetra-ubiquitin chains (Enzo Life Science) in 400 μL of cold buffer (50 mM Tris·HCl at pH 7.5, 150 mM NaCl, 10 mM $MgCl_2$, 0.05% Tween-20) under rotation at 4 °C. The beads were then washed four times with cold buffer, proteins were eluted with 40 mM glutathione, and bead-bound materials were subjected to SDS/PAGE and analyzed by immunoblotting.

For the ubiquitin-binding assay with plant total extracts, 6 g of *Arabidopsis* seedlings was ground and homogenized in 10 mL of lysis buffer A (50 mM Tris·HCl at pH 7.5, 100 mM NaCl, 10% glycerol), supplemented with 0.2% Triton X-100 and 1× protease inhibitor mixture (Roche), and clarified by centrifugation for 15 min at 13,000 × *g*. The supernatant was mixed with 400 μg of bead-bound GST or GST-SH3P2(SH3) and incubated for 6 h at 4 °C with gentle rotation. Samples were washed four times in buffer A and eluted by boiling in 1× SDS sample buffer. Samples were separated by SDS/PAGE and analyzed by immunoblotting.

Immunoprecipitations. One gram of 7-d-old seedlings was ground and homogenized in 2 mL of buffer A (50 mM Tris·HCl at pH 7.5, 100 mM NaCl, 10% glycerol) supplemented with 0.2% Nonidet P-40 and 1× protease inhibitor mixture. Cell lysates were clarified by centrifugation for 15 min at 13,000 × *g*, diluted 10-fold with buffer A, and incubated with GFP-TRAP Magnetic Agarose Beads (ChromoTek) for 1.5 h at 4 °C while rotating. Samples were washed four times in buffer A and eluted by boiling in 30 μL of 1× SDS sample buffer before being subjected to SDS/PAGE and immunoblotting analysis.

ACKNOWLEDGMENTS. We thank Akihiko Nakano, Takashi Ueda, Tomohiro Uemura, and Masaru Fujimoto (The University of Tokyo) for the endosomal marker lines and Sven Schellmann and Martin Hülskamp (University of Cologne) for the VPS23.1-HA (ELCH-HA) line. We thank Stefan Helfrich and the Bioimaging Center (University of Konstanz) for support in image analysis. We thank the Nottingham Arabidopsis Stock Center (NASC) for providing *Arabidopsis* T-DNA insertion lines. This work was supported by Grants IS 221/2-1, IS 221/4-1, and SFB924(A6) from the German Science Foundation (to E.I.); European cooperation in science and technology (COST) Action BM1307 [COST-proteostasis (to E.I.)]; Grant 1121998 from the National Science Foundation (to S.Y.B.); and Grant 16H05068 from the Ministry of Education, Culture, Sports, Science and Technology Japan (to M.H.S.).

1. Vierstra RD (2012) The expanding universe of ubiquitin and ubiquitin-like modifiers. *Plant Physiol* 160:2–14.
2. Ben Khaled S, Postma J, Robatzek S (2015) A moving view: Subcellular trafficking processes in pattern recognition receptor-triggered plant immunity. *Annu Rev Phytopathol* 53:379–402.
3. Paez Valencia J, Goodman K, Otegui MS (2016) Endocytosis and endosomal trafficking in plants. *Annu Rev Plant Biol* 67:309–335.
4. McMahon HT, Boucrot E (2011) Molecular mechanism and physiological functions of clathrin-mediated endocytosis. *Nat Rev Mol Cell Biol* 12:517–533.
5. Baisa GA, Mayers JR, Bednarek SY (2013) Budding and braking news about clathrin-mediated endocytosis. *Curr Opin Plant Biol* 16:718–725.
6. Robinson MS (2015) Forty years of clathrin-coated vesicles. *Traffic* 16:1210–1238.
7. Komander D, Rape M (2012) The ubiquitin code. *Annu Rev Biochem* 81:203–229.
8. Lauwers E, Jacob C, André B (2009) K63-linked ubiquitin chains as a specific signal for protein sorting into the multivesicular body pathway. *J Cell Biol* 185:493–502.
9. Leitner J, et al. (2012) Lysine63-linked ubiquitylation of PIN2 auxin carrier protein governs hormonally controlled adaptation of *Arabidopsis* root growth. *Proc Natl Acad Sci USA* 109:8322–8327.
10. Martins S, et al. (2015) Internalization and vacuolar targeting of the brassinosteroid hormone receptor BRI1 are regulated by ubiquitination. *Nat Commun* 6:6151.
11. Barberon M, et al. (2011) Monoubiquitin-dependent endocytosis of the iron-regulated transporter 1 (IRT1) transporter controls iron uptake in plants. *Proc Natl Acad Sci USA* 108:E450–E458.
12. Kasai K, Takano J, Miwa K, Toyoda A, Fujiwara T (2011) High boron-induced ubiquitination regulates vacuolar sorting of the BOR1 borate transporter in *Arabidopsis thaliana*. *J Biol Chem* 286:6175–6183.
13. Göhre V, et al. (2008) Plant pattern-recognition receptor FLS2 is directed for degradation by the bacterial ubiquitin ligase AvrPtoB. *Curr Biol* 18:1824–1832.
14. Gimenez-Ibanez S, et al. (2009) AvrPtoB targets the LysM receptor kinase CERK1 to promote bacterial virulence on plants. *Curr Biol* 19:423–429.
15. Winter V, Hauser MT (2006) Exploring the ESCRTing machinery in eukaryotes. *Trends Plant Sci* 11:115–123.
16. Henne WM, Buchkovich NJ, Emr SD (2011) The ESCRT pathway. *Dev Cell* 21:77–91.
17. Strack B, Calistri A, Craig S, Popova E, Göttlinger HG (2003) AIP1/ALIX is a binding partner for HIV-1 p6 and EIAV p9 functioning in virus budding. *Cell* 114:689–699.
18. von Schwedler UK, et al. (2003) The protein network of HIV budding. *Cell* 114:701–713.
19. Olmos Y, Hodgson L, Mantell J, Verkade P, Carlton JG (2015) ESCRT-III controls nuclear envelope reformation. *Nature* 522:236–239.
20. Vietri M, et al. (2015) Spastin and ESCRT-III coordinate mitotic spindle disassembly and nuclear envelope sealing. *Nature* 522:231–235.

21. Denais CM, et al. (2016) Nuclear envelope rupture and repair during cancer cell migration. *Science* 352:353–358.
22. Raab M, et al. (2016) ESCRT III repairs nuclear envelope ruptures during cell migration to limit DNA damage and cell death. *Science* 352:359–362.
23. Gong YN, et al. (2017) ESCRT-III acts downstream of MLKL to regulate necroptotic cell death and its consequences. *Cell* 169:286–300.e216.
24. Shields SB, Piper RC (2011) How ubiquitin functions with ESCRTs. *Traffic* 12:1306–1317.
25. Ren X, Hurley JH (2010) VHS domains of ESCRT-0 cooperate in high-avidity binding to polyubiquitinated cargo. *EMBO J* 29:1045–1054.
26. Korbei B, et al. (2013) *Arabidopsis* TOL proteins act as gatekeepers for vacuolar sorting of PIN2 plasma membrane protein. *Curr Biol* 23:2500–2505.
27. Puertollano R, Bonifacino JS (2004) Interactions of GGA3 with the ubiquitin sorting machinery. *Nat Cell Biol* 6:244–251.
28. Puertollano R (2005) Interactions of TOM1L1 with the multivesicular body sorting machinery. *J Biol Chem* 280:9258–9264.
29. Belda-Palazon B, et al. (2016) FYVE1/FREE1 interacts with the PYL4 ABA receptor and mediates its delivery to the vacuolar degradation pathway. *Plant Cell* 28:2291–2311.
30. Gao C, et al. (2014) A unique plant ESCRT component, FREE1, regulates multivesicular body protein sorting and plant growth. *Curr Biol* 24:2556–2563.
31. Gao C, et al. (2015) Dual roles of an *Arabidopsis* ESCRT component FREE1 in regulating vacuolar protein transport and autophagic degradation. *Proc Natl Acad Sci USA* 112:1886–1891.
32. Kolb C, et al. (2015) FYVE1 is essential for vacuole biogenesis and intracellular trafficking in *Arabidopsis*. *Plant Physiol* 167:1361–1373.
33. Zhuang X, et al. (2013) A BAR-domain protein SH3P2, which binds to phosphatidylinositol 3-phosphate and ATG8, regulates autophagosome formation in *Arabidopsis*. *Plant Cell* 25:4596–4615.
34. Lam BC, Sage TL, Bianchi F, Blumwald E (2001) Role of SH3 domain-containing proteins in clathrin-mediated vesicle trafficking in *Arabidopsis*. *Plant Cell* 13:2499–2512.
35. Ahn G, et al. (2017) SH3P2 plays a crucial role at the step of membrane tubulation during cell plate formation in plants. *Plant Cell* 29:1388–1405.
36. Ortega Roldan JL, et al. (2013) Distinct ubiquitin binding modes exhibited by SH3 domains: Molecular determinants and functional implications. *PLoS One* 8: e73018.
37. Stamenova SD, et al. (2007) Ubiquitin binds to and regulates a subset of SH3 domains. *Mol Cell* 25:273–284.
38. Willige BC, et al. (2007) The DELLA domain of GA INSENSITIVE mediates the interaction with the GA INSENSITIVE DWARF1A gibberellin receptor of *Arabidopsis*. *Plant Cell* 19:1209–1220.
39. Scheuring D, et al. (2011) Multivesicular bodies mature from the trans-Golgi network/early endosome in *Arabidopsis*. *Plant Cell* 23:3463–3481.
40. Uemura T, et al. (2012) Qa-SNAREs localized to the trans-Golgi network regulate multiple transport pathways and extracellular disease resistance in plants. *Proc Natl Acad Sci USA* 109:1784–1789.
41. Geldner N, et al. (2009) Rapid, combinatorial analysis of membrane compartments in intact plants with a multicolor marker set. *Plant J* 59:169–178.
42. Reynolds GD, August B, Bednarek SY (2014) Preparation of enriched plant clathrin-coated vesicles by differential and density gradient centrifugation. *Methods Mol Biol* 1209:163–177.
43. Tanaka N, et al. (1999) Possible involvement of a novel STAM-associated molecule "AMSH" in intracellular signal transduction mediated by cytokines. *J Biol Chem* 274: 19129–19135.
44. Kalinowska K, et al. (2015) *Arabidopsis* ALIX is required for the endosomal localization of the deubiquitinating enzyme AMSH3. *Proc Natl Acad Sci USA* 112:E5543–E5551.
45. Yu F, et al. (2016) ESCRT-I component VPS23A affects ABA signaling by recognizing ABA receptors for endosomal degradation. *Mol Plant* 9:1570–1582.
46. Mayer BJ (2001) SH3 domains: Complexity in moderation. *J Cell Sci* 114:1253–1263.
47. Zarrinpar A, Bhattacharyya RP, Lim WA (2003) The structure and function of proline recognition domains. *Sci STKE* 2003:RE8.
48. Spitzer C, et al. (2006) The *Arabidopsis elch* mutant reveals functions of an ESCRT component in cytokinesis. *Development* 133:4679–4689.
49. Wang HJ, et al. (2017) VPS36-dependent multivesicular bodies are critical for plasmamembrane protein turnover and vacuolar biogenesis. *Plant Physiol* 173:566–581.
50. Lu D, et al. (2011) Direct ubiquitination of pattern recognition receptor FLS2 attenuates plant innate immunity. *Science* 332:1439–1442.
51. Shin LJ, et al. (2013) IRT1 degradation factor1, a ring E3 ubiquitin ligase, regulates the degradation of iron-regulated transporter1 in *Arabidopsis*. *Plant Cell* 25:3039–3051.
52. McCullough J, et al. (2006) Activation of the endosome-associated ubiquitin isopeptidase AMSH by STAM, a component of the multivesicular body-sorting machinery. *Curr Biol* 16:160–165.
53. Spallek T, et al. (2013) ESCRT-I mediates FLS2 endosomal sorting and plant immunity. *PLoS Genet* 9:e1004035.
54. Isono E, et al. (2010) The deubiquitinating enzyme AMSH3 is required for intracellular trafficking and vacuole biogenesis in *Arabidopsis thaliana*. *Plant Cell* 22:1826–1837.
55. Hummel E, Osterrieder A, Robinson DG, Hawes C (2010) Inhibition of Golgi function causes plastid starch accumulation. *J Exp Bot* 61:2603–2614.
56. Raiborg C, et al. (2002) Hrs sorts ubiquitinated proteins into clathrin-coated microdomains of early endosomes. *Nat Cell Biol* 4:394–398.
57. Raiborg C, Wesche J, Malerød L, Stenmark H (2006) Flat clathrin coats on endosomes mediate degradative protein sorting by scaffolding Hrs in dynamic microdomains. *J Cell Sci* 119:2414–2424.
58. Sachse M, Urbé S, Oorschot V, Strous GJ, Klumperman J (2002) Bilayered clathrin coats on endosomal vacuoles are involved in protein sorting toward lysosomes. *Mol Biol Cell* 13:1313–1328.
59. Spitzer C, et al. (2009) The ESCRT-related CHMP1A and B proteins mediate multivesicular body sorting of auxin carriers in *Arabidopsis* and are required for plant development. *Plant Cell* 21:749–766.
60. Clough SJ, Bent AF (1998) Floral dip: A simplified method for *Agrobacterium*-mediated transformation of *Arabidopsis thaliana*. *Plant J* 16:735–743.
61. Katsiarimpa A, et al. (2011) The *Arabidopsis* deubiquitinating enzyme AMSH3 interacts with ESCRT-III subunits and regulates their localization. *Plant Cell* 23:3026–3040.
62. Nakagawa T, et al. (2007) Development of series of gateway binary vectors, pGWBs, for realizing efficient construction of fusion genes for plant transformation. *J Biosci Bioeng* 104:34–41.
63. Shimada TL, Shimada T, Hara-Nishimura I (2010) A rapid and non-destructive screenable marker, FAST, for identifying transformed seeds of *Arabidopsis thaliana*. *Plant J* 61:519–528.
64. Grefen C, et al. (2010) A ubiquitin-10 promoter-based vector set for fluorescent protein tagging facilitates temporal stability and native protein distribution in transient and stable expression studies. *Plant J* 64:355–365.
65. Ito E, et al. (2012) Dynamic behavior of clathrin in *Arabidopsis thaliana* unveiled by live imaging. *Plant J* 69:204–216.
66. Katsiarimpa A, et al. (2013) The deubiquitinating enzyme AMSH1 and the ESCRT-III subunit VPS2.1 are required for autophagic degradation in *Arabidopsis*. *Plant Cell* 25: 2236–2252.
67. Kushnirov VV (2000) Rapid and reliable protein extraction from yeast. *Yeast* 16: 857–860.
68. Schindelin J, et al. (2012) Fiji: An open-source platform for biological-image analysis. *Nat Methods* 9:676–682.